Rippling pattern of distortion product otoacoustic emissions evoked by high-frequency primaries in guinea pigs

George W.S. Burwood[a)], Ian J. Russell, Andrei N. Lukashkin[b)]

Sensory Neuroscience Research Group, School of Pharmacy and Biomolecular Sciences, University of Brighton, Brighton, BN2 4GJ, UK

[a)]Current address: Oregon Hearing Research Center, Oregon Health and Science University, 3181 SW Sam Jackson Park Rd, Portland, Oregon 97239, USA

Short title: High-frequency emissions in guinea pigs

[b)]Corresponding Author:

Andrei N. Lukashkin

School of Pharmacy and Biomolecular Sciences

Huxley Building, University of Brighton

Lewes Road, Brighton, BN2 4GJ, UK

Tel: +44 1273 642103

E-mail: a.lukashkin@brighton.ac.uk

ABSTRACT

The origin of ripples in DPOAE amplitude which appear at specific DPOAE frequencies during f_1 tone sweeps using fixed high frequency f_2 (>20kHz) in guinea pigs is investigated. The peaks of the ripples, or local DPOAE amplitude maxima, are separated by approximately half octave intervals and are accompanied by phase oscillations. The local maxima appear at the same frequencies in DPOAEs of different order and velocity responses of the stapes and do not shift with increasing levels of the primaries. A suppressor tone had little effect on the frequencies of the maxima, but partially suppressed DPOAE amplitude when it was placed close to the f_2 frequencies. These findings agree with earlier observations that the maxima occur at the same DPOAE frequencies, which are independent of the f_2 and the primary ratio, and thus are likely to be associated with DPOAE propagation mechanisms. Furthermore, the separation of the local maxima by approximately half an octave may suggest that they are due to interference of the travelling waves along the basilar membrane at the frequency of the DPOAE. It is suggested that the rippling pattern appears because of interaction between DPOAE reverse travelling waves with standing waves formed in the cochlea.

I. INTRODUCTION

The behaviour of the amplitude and phase of distortion product otoacoustic emissions (DPOAEs) generated by the cochlea during two-tone stimulation (Kemp, 1979) is complex. The DPOAE amplitude and phase behaviour depends on the animal species and the frequencies, levels, and separation of the primary tones (f_1 and f_2, $f_2>f_1$). Many characteristics of DPOAEs and their generation mechanisms have been explored, including the existence of DPOAE fine structure, the non-monotonic behaviour of emissions as a function of frequency and level of the primaries, and band pass filtering produced as a function of primary frequency ratio (for review see Avan *et al*., 2013). However, a complete understanding of DPOAE generation and propagation is still lacking.

There is a general consensus that DPOAEs recorded in the ear canal are the vector sums of emissions generated by at least two sources (Brown *et al*., 1996; Shera and Guinan, 1999; Talmadge *et al*., 1999, Knight and Kemp, 2000; Kalluri and Shera, 2001). One source is the overlap between the two primary tones (Russell and Nilsen, 1997), where energy at the distortion frequencies is produced (Brown and Kemp, 1984) and elicits a travelling wave in the forward and reverse directions. The forward travelling wave peaks closer to the apex of the cochlea at the distortion characteristic frequency (CF) place, and is partially reflected back out of the cochlea, due to random mechanical irregularities along the organ of Corti (Kemp and Brown, 1983; Hilger *et al*., 1995; Zweig and Shera, 1995; Shera and Guinan, 1999; Konrad-Martin *et al*., 2001). The mixing of these two emissions, so called distortion-source and reflection-source emissions, has been shown to cause fine structure of DPOAE recorded in the ear canal (Heitmann *et al*., 1998; Talmadge *et al*., 1999). However, such mechanical irregularities putatively responsible for generation of reflection-source emission are less prominent in rodents (Kemp, 1986; Lonsbury-Martin *et al*., 1988; Shera and Guinan, 1999), and DPOAEs measured in rodent species do not display the rapidly changing fine

structure of human DPOAEs (Withnell *et al*., 2003). This observation has led to a debate as to the mechanism behind the non-monotonic changes in DPOAE amplitudes during changes of the primary frequencies in non-human mammal species (Lukashkin and Russell, 2001; Withnell *et al*., 2003; Goodman *et al*., 2003; Lukashkin *et al*., 2007; de Boer *et al*., 2007).

The rippling of the DPOAE amplitude with distinct local maxima observed for specific DPOAE frequencies when the primary frequency ratio f_2/f_1 is varied and f_2 is kept constant have been described (Lukashkin *et al*., 2007). These local amplitude maxima appeared at similar frequencies for moderate sound pressure levels across animals of the same species and across different f_2 frequencies. Maxima at similar frequencies were also reported when measuring higher order emissions ($3f_1$-$2f_2$ and $4f_1$-$3f_2$). The finding that the local amplitude maxima were observed at the same DPOAE frequencies in emissions of different orders and, hence, for different primary ratios indicates that these maxima may be related to the propagation rather than the generation of DPOAEs. It was suggested (Lukashkin *et al*., 2007) that this rippling pattern may be due to formation of standing waves in the cochlea (Kemp, 1979; Russell and Kössl, 1999; Goodman *et al*., 2003; Shera, 2003). Cochlear standing waves may form during the DPOAE back propagation as a slow wave (Vetešník and Gummer, 2012), with the possibility that, in a variety of experimental paradigms, the formation of standing waves can contribute to the non-monotonic behaviour of DPOAE amplitude.

In this paper we further investigate the rippling, non-monotonic behaviour of the distortion product amplitude in acoustic responses of the cochlea and mechanical responses of the stapes during variation of the primary frequency ratio and levels of the primary tones, and in the presence of a suppressor tone. It is concluded that local DPOAE amplitude maxima are due to formation of cochlear standing waves.

II. METHODS

A. Animal preparation

Data collected from 9 pigmented guinea pigs (male and female 172-393g) was used in this study. DPOAE data were collected from 4 animals and a further 5 animals were used for combined recording of DPOAE and mechanical responses of the stapes. All procedures involving animals were performed in accordance with UK Home Office regulations with approval from the University of Brighton Animal Welfare and Ethical Review Body. Guinea pigs were anaesthetised with the neurolept anaesthetic technique, (0.06 mg/kg body weight atropine sulphate s.c., 30mg/kg pentobarbital i.p., and 500 µl/kg Hypnorm i.m.). Additional injections of Hypnorm were given every 40 minutes at half of the initial dose. Additional doses of pentobarbital were administered as needed to maintain a non-reflexive state. The heart rate was monitored with a pair of skin electrodes placed on both sides of the thorax. The animals were tracheotomised and artificially ventilated, and their core temperature was maintained at 38ºC with a heating blanket and heated head holder. The middle ear cavity was opened to reveal the round window and the middle ear ossicles.

B. Sound stimulation and DPOAE recording

Sound was delivered to the tympanic membrane by a closed acoustic system comprising of two Bruel & Kjaer 4131 ½-inch speakers for delivering tones and a single Bruel & Kjaer 3133 ½ inch microphone for monitoring sound pressure. The sound system was coupled to the ear canal via 1 cm long, 4 cm diameter tubes to a conical speculum, the 1 mm diameter opening of which was placed about 1 mm from the tympanic membrane. The closed sound system was calibrated in situ for frequencies between 1 and 50 kHz. Known sound-pressure levels were expressed in dB SPL re: 2×10^{-5} Pa. All sound stimuli in this work were shaped with raised cosines of 0.5 ms in duration at the beginning and end of stimulation. White noise for acoustical calibration and tone sequences for auditory stimulation were synthesised by a

Data Translation 3010 board at a sampling rate of 250 kHz and delivered to the microphones through low-pass filters (100 kHz cut-off frequency). Signals from the measuring amplifier were digitized at 250 kHz using the same board and averaged in the time domain. Amplitudes of the spectral maxima were obtained by performing an FFT on a time domain averaged signal, 4096 points in length. The maximum level of system distortion measured with an artificial ear cavity for the highest levels of primaries used in this study (L_1=70 dB SPL) was 70 dB below the primary level.

DPOAE ratio functions were recorded using f_1 sweeps with constant f_2. Levels of the primaries, L_1 and L_2, were constant during each sweep with L_1=L_2+10 dB. For suppression experiments, a calibrated 67 dB SPL suppressor tone was added using a Philips PM1593 programmable function generator, and ratio functions were recorded in the presence of different suppressor frequencies. The simultaneous suppression paradigm was implemented. The suppressor was presented over the duration of the primaries.

C. Recording of stapes vibrations

Stapes vibrations were recorded using a CLV-2534 Laser Vibrometer (Polytec, Germany). The laser beam was focussed onto the incudostapedial joint, or the head of the stapes, depending upon target angle and accessibility in individual preparations. No noticeable difference between the two recording sites was observed. Care was taken throughout data acquisition to maintain the highest reflected signal possible, by adjusting the focus of the laser point to account for gross physiological movement within the preparation. The output voltage from the vibrometer was band-pass filtered between 100 Hz – 100 kHz, with a sensitivity of 2mm/s/V and a gain of x100.

Experimental control and data acquisition were performed using a PC with custom programs written in MATLAB (MathWorks, MA). Data analysis was performed using Origin

(OriginLab, MA). Acoustic and laser measurements were conducted in healthy cochleae, and post mortem following overdose using Euthatal, in the presence of sodium salicylate crystals placed onto the round window membrane.

III. RESULTS

The DPOAE amplitude as a function of primary frequency ratio has a well-known bell-like shape (e.g. Brown *et al*., 1992) when constant f_2 is in the low-/mid-frequency range for guinea pigs (Fig. 1). The maximum of this bell-like shape is observed at approximately the same frequency for DPOAEs of different order (Fig. 1), where the order of DPOAE mf_1+nf_2 is determined by the sum m+n. The position of this maximum is level dependent and it shifts towards lower frequencies with increasing level of the primaries (Lukashkin and Russell, 2001; Lukashkin et al., 2007).

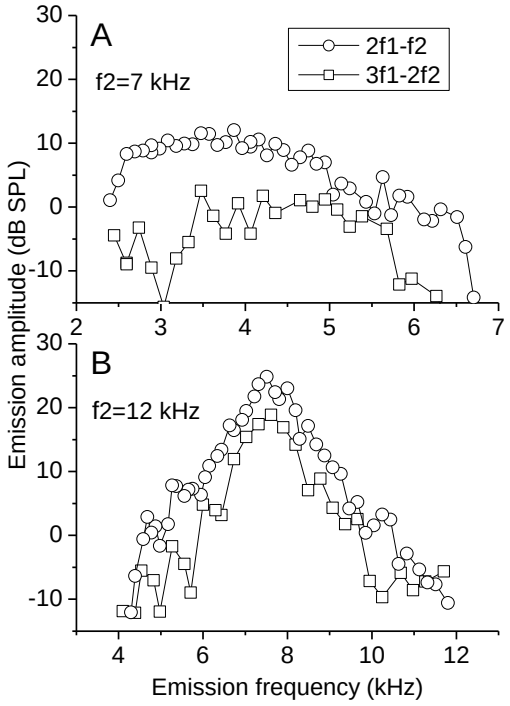

FIG. 1. Dependence of DPOAE amplitude on the f_2/f_1 ratio for low-frequency primaries in a single preparation. Symbol coding for different DPOAEs is shown at the top panel. f_2 was fixed and its value is indicated within the panels; f_1 was varied to obtain the required DPOAE frequency. Primary levels were fixed at $L_1 = L_2+10$ dB=40 dB SPL.

This dependence, however, becomes more complex for high-frequency primaries, namely local amplitude maxima are superimposed onto the general bell-like shape when constant f_2 is kept above 12 kHz (Lukashkin *et al*., 2007). The local maxima generated for f_2 at and above 24 kHz are marked as X, Y and Z in Figure 2.

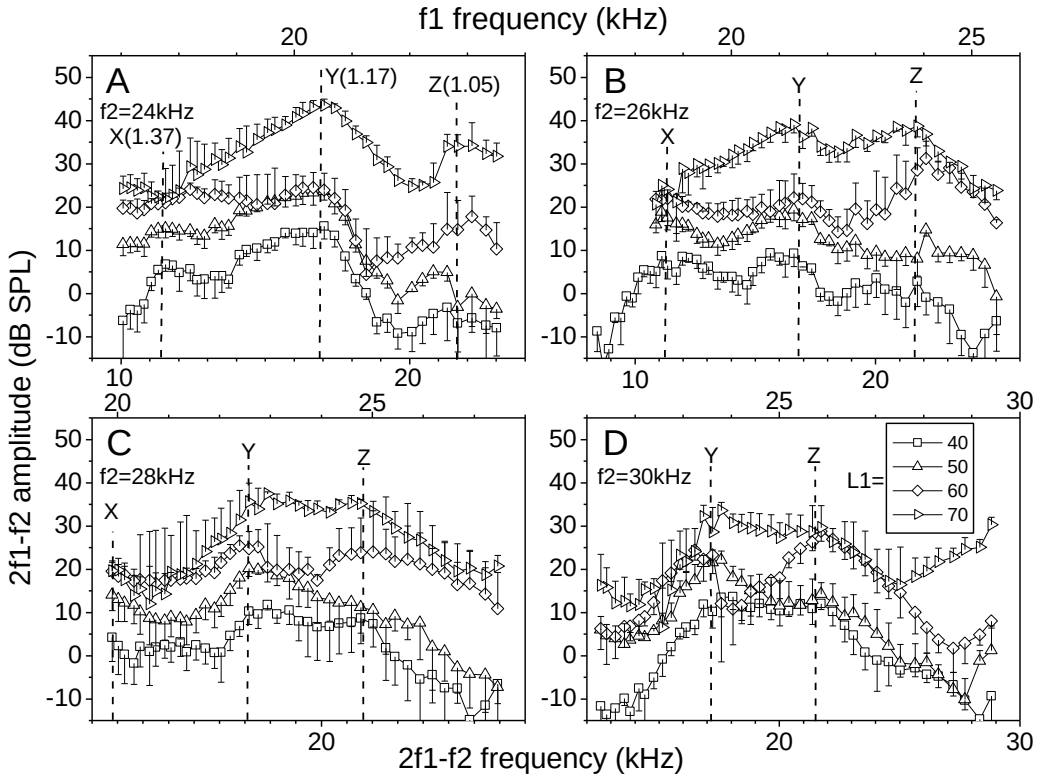

FIG. 2. Dependence of $2f_1$-f_2 amplitude (mean ± SD, n=4) on the f_2/f_1 ratio for different high-frequency f_2 and different levels of stimulation. Corresponding fixed values of f_2 are indicated within each panel; f_1 (top abscissa) was varied to obtain the required DPOAE frequency. Primary levels were fixed for each curve at $L_1 = L_2$+10 dB. Symbol coding for different L_1 is shown at the bottom right panel. Vertical dashed line indicate the approximate positions of local amplitude maxima denoted as X, Y and Z. The f_2/f_1 ratio for the positions of the dashed lines in A-D is indicated in brackets in A (top left).

Regardless of f_2 value, the maxima remain at approximately the same frequency but, because of presence of the general bell-like shape, their position may shift slightly for different parameters of stimulation. These local amplitude maxima are separated by approximately half-octave intervals. The maxima may not be pronounced at intermediate levels of the

primaries due to non-monotonic growth of the DPOAE amplitude (Lukashkin and Russell, 1999; Lukashkin et al., 2002), but they reappear at higher levels of the primaries. The phase

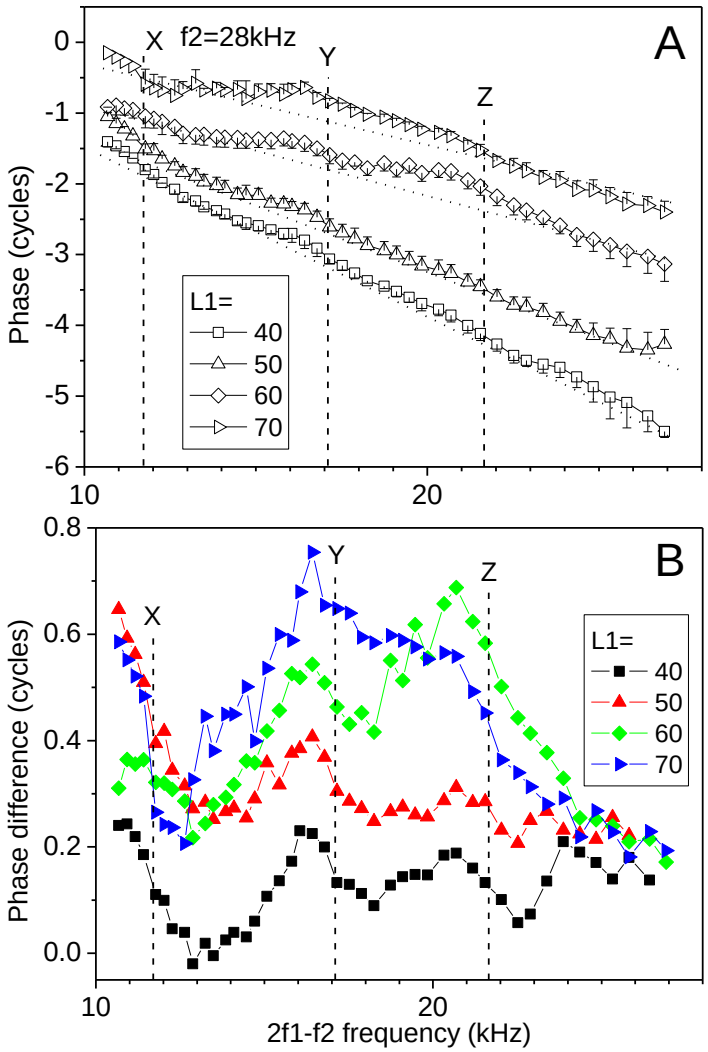

FIG. 3. (color online) Phase behaviour of high-frequency DPOAE. A. Dependence of $2f_1$-f_2 phase (mean ± SD, n=4) on the f_2/f_1 ratio for different levels of stimulation. B. Phase difference between phase plots in A and corresponding constant slopes indicated by dashed lines in A. f_2 was fixed at 28 kHz. Primary levels were fixed for each curve at $L_1 = L_2+10$ dB. Symbol coding for different L_1 is shown within each panel. Vertical dashed lines are situated at the same frequencies as in Fig. 2C and indicate approximate positions of amplitude maxima denoted as X, Y and Z. Phase was corrected for the primary phases and phase transitions (up to half-cycle) associated with the amplitude notch due to DPOAE generating non-linearity (Lukashkin and Russell, 1999).

of the high-frequency DPOAEs shows associated oscillations (illustrated for f_2=28 kHz in

Fig. 3) which occur with the same periodicity as the amplitude maxima. Similar phase patterns are usually observed during wave interaction and may indicate the amplitude maxima originate from the summation of waves at the DPOAE frequencies.

It is worth noting that the amplitude maxima are observed for the same DPOAE frequencies, and, hence, for different primary ratios and different corresponding f_1, in both distortion components ($2f_1$-f_2, $3f_1$-$2f_2$) analysed in this paper (Fig. 4). It has been observed previously that the $4f1$-$3f2$ emission contains these frequency specific maxima (Lukashkin *et al*. 2007).

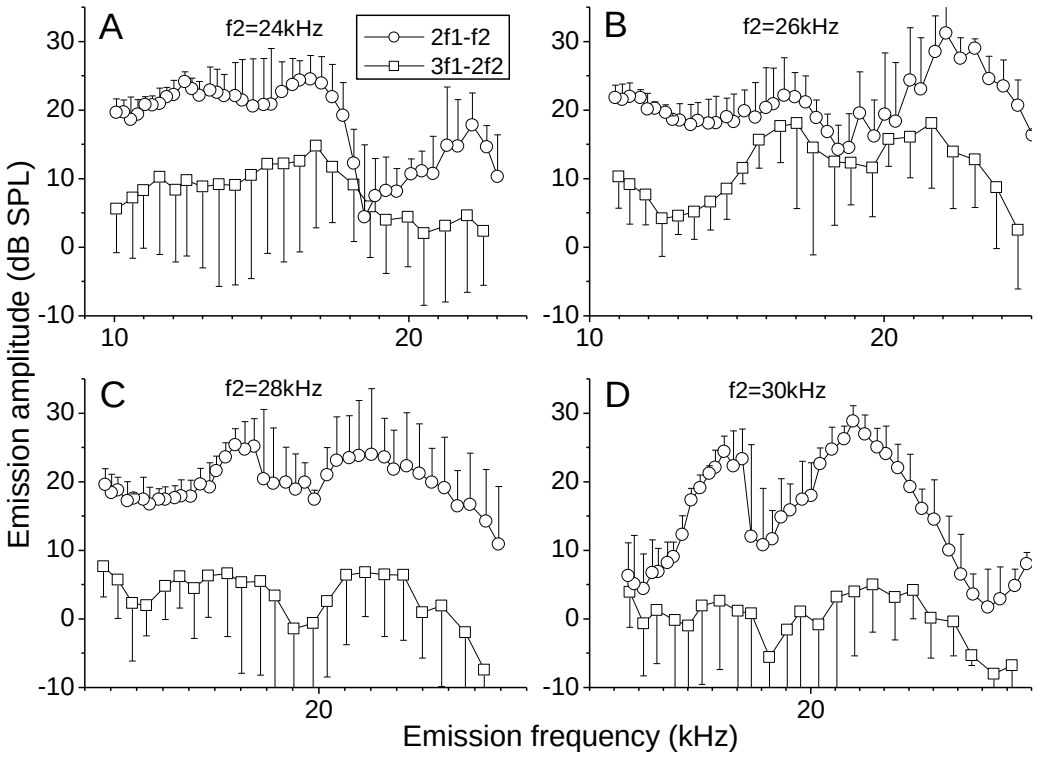

FIG. 4. Dependence of DPOAE amplitude (mean ± SD, n=4) on the f_2/f_1 ratio for different high-frequency f_2. Corresponding fixed values of f_2 are indicated within each panel; f_1 was varied to obtain the required DPOAE frequency. Primary levels were fixed at $L_1 = L_2$+10 dB=50 dB SPL. Symbol coding for different orders of DPOAEs is shown in A.

For low levels of the primaries, the amplitude notches between the maxima are less pronounced but the maxima are still visible. The maximum amplitude of the bell-like shape of DPOAEs shifts to lower frequencies with increasing level of the primaries (e.g. see

Lukashkin and Russell, 2001; Lukashkin *et al*., 2007). There is, however, no statistically significant (p = 0.05) shift in the frequency of the local amplitude maxima with increasing level of the primaries (Fig. 5).

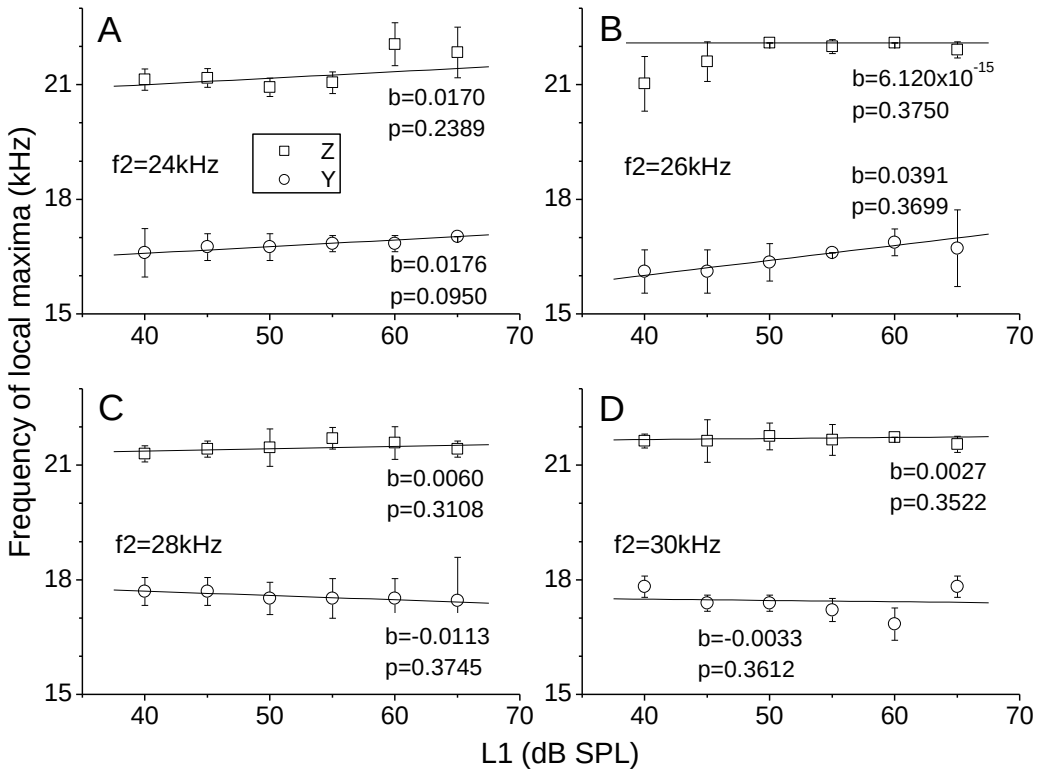

FIG. 5. Dependence of position of local amplitude maxima on level of the primaries for different high-frequency f_2. Data points show average values for 4 preparations (mean ± SD). Corresponding fixed values of f_2 are indicated within each panel. Symbol coding for maxima Y and Z (the same notation as in Fig. 2) is shown at the top left panel. Straight lines indicate linear regressions fit to the data. Slopes (b) of the linear regression fit and calculated p-values for the regression slope analysis (two-tailed t-test; null hypothesis: the slope of the regression line is equal to zero; 95% confidence level) are indicated near each line.

To confirm that the rippling pattern of the DPOAE amplitude is of cochlear origin, stapes velocity at the $2f_1$-f_2 frequency in healthy and passive cochleae was recorded. Figure 6 shows both the DPOAE amplitude and the velocity of the stapes vibrations at the $2f_1$-f_2 frequency in

healthy cochleae and post mortem in the presence of salicylate to block the residual OHC somatic motility (Dieler *et al*., 1991).

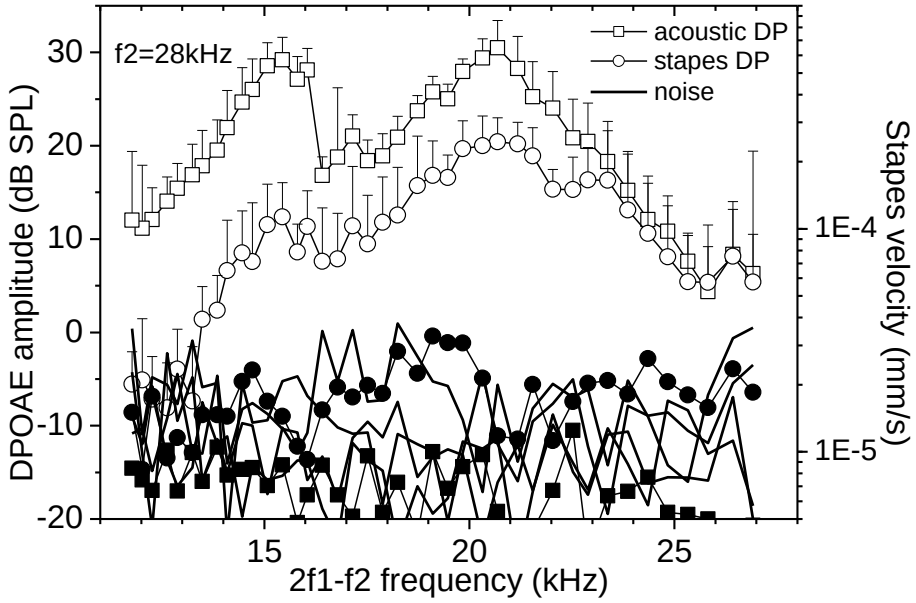

FIG. 6. Dependence of the DPOAE amplitude (squares) and the velocity of the stapes vibrations (circles) at the $2f_1$-f_2 frequency (mean ± SD, n=5) on the f_2/f_1 ratio. f_2 was fixed at 28 kHz. Primary levels were fixed at $L_1 = L_2$+10 dB=50 dB SPL. Solid symbols indicate post mortem responses in the presence of salicylate. Black lines indicate corresponding noise floors.

The local maxima in the DPOAE amplitude and in the stapes distortion products were conserved between the two measurement techniques. The low frequency maximum in the stapes responses was relatively lower in amplitude than that recorded acoustically. This could be due to multimodal vibrations of the stapes, whereby at low frequencies it moves in a single, piston-like mode, but at higher frequencies displays complex rocking motion (e.g. Eiber *et al*., 2012). Because the stapes response was recorded in a single plane in our experiments, summation of energy of these different modes at the level of the acoustic response (DPOAE) in the ear canal could produce a relatively larger overall response. In post mortem preparations where OHC somatic motility was additionally suppressed by salicylate,

195 both the DPOAE amplitude and the amplitude of distortion products of the stapes velocity
196 responses dropped into the noise floor. This indicates that the local maxima in the primary
197 ratio functions are of cochlea origin and physiologically vulnerable.

198 To examine whether the rippling pattern of the DPOAE amplitude was due to interaction
199 between emissions from the distortion source and the reflection source, a third, suppressor
200 tone which spanned a wide range of frequencies was added to the acoustic stimulation. When
201 the suppressor tone was added, it changed the dependence of the DPOAE amplitude on the
202 ratio of the primaries (Fig. 7).

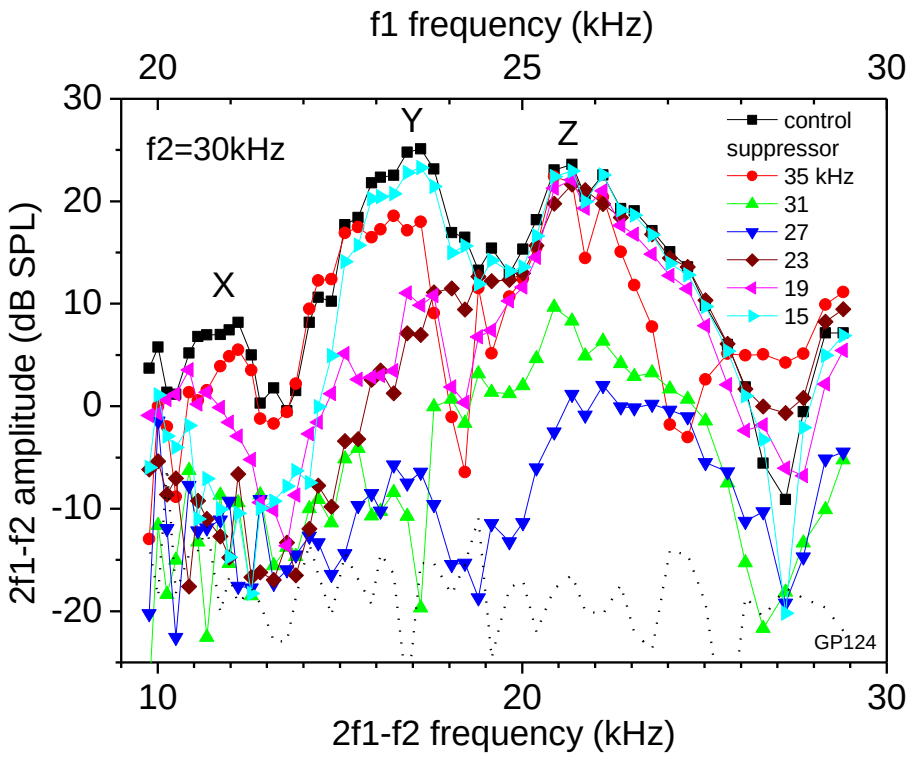

FIG. 7. (color online) Dependence of $2f_1$-f_2 amplitude on the f_2/f_1 ratio for different frequencies of the suppressor tone recorded in a single preparation. f_2 was fixed at 30 kHz. Primary levels were fixed at $L_1 = L_2$+10 dB =60 dB SPL. Black squares indicate response in the absence of suppressor. The suppressor level was fixed for all curves at 67 dB SPL. Suppressor frequency was fixed for each f_2/f_1 ratio curve and is indicated within the figure legend. The local amplitude maxima are labelled X, Y and Z (the same notation as in Fig. 2). The top abscissa shows corresponding f_1 frequencies. Dotted line shows the noise floor.

Suppressor tones close to f_2 (27 and 31 kHz in Fig. 7) were the most efficient in decreasing the overall DPOAE amplitude over a wide frequency range. Presumably, because these suppressors effectively suppress responses of both primaries in the region of their overlap. For all frequencies of the suppressor, the absolute decrease of the DPOAE amplitude was, however, larger for the low-frequency shoulder of the ratio dependence and, hence, low-frequency maxima X and Y were suppressed more efficiently than maximum Z. Peak Z was reduced in the presence of the suppressor only when the suppressor frequency was close to f_2.

Maxima X and Y were also affected by suppressors close to the f_2, but there appeared to be little evidence of a functional relationship between suppressor frequency and suppression efficiency for lower frequencies. Whilst the observation that suppression is more efficient for suppressor tones closer in frequency to f_2 is well supported (Brown and Kemp, 1984; Harris *et al*., 1992; Kummer *et al*., 1995; Abdala *et al*., 1996; Martin *et al*., 1998), the finding that the absolute decrease of the DPOAE amplitude was larger for the low-frequency shoulder of the ratio dependence may be somewhat counterintuitive. This effect can be explained by considering the responses of the primaries in the region of their overlap, which is close to the f_2 place and is thought to be the region where energy at the distortion is originally produced (Brown and Kemp, 1984). The low-frequency suppressor tone's effect (15 and 19 kHz suppressor, Fig. 7) on the DPOAE amplitude would be relatively small for small f_2/f_1 ratios when the primary frequencies are close to each other and produce large responses in the overlap region. When primary frequency separation increases, the suppressor becomes effective against f_1 when f_1 is further away from f_2 and when responses of the suppressor and f_1 in the primary overlap region become comparable. Significantly for this study, there was no local suppression effect observed for maxima X, Y and Z whilst the suppressor frequency was close to the $2f_1$-f_2, hence, contribution of the secondary emission source into the generation of the local amplitude maxima was minimal.

IV. DISCUSSION

This study investigates the origin of ripples in the amplitude of high-frequency DPOAEs which form local amplitude maxima at specific DPOAE frequencies independent of the primary frequencies and levels. The maxima are separated by approximately half octave intervals and they are observed at the same frequencies in the DPOAEs of different order and, in fact, in responses of the stapes at the distortion frequencies. A third high-level tone, while

suppressing overall amplitude of the DPOAE, does not suppress this rippling pattern whether the suppressor frequency is close to f_1, f_2 or to the frequency of emission.

The rippling pattern is generated within the cochlea and is already seen in the stapes vibrations at the corresponding frequencies. Logarithmic scaling of these frequencies resembles the cochlear logarithmic scaling (von Békésy, 1960; Greenwood, 1990), which makes it unlikely that the local maxima are artefacts of the acoustic systems used for DPOAE stimulation and recording. The frequencies of the local maxima appear to be due to the intrinsic characteristics of the guinea pig cochlea because these frequencies do not depend on the primary frequencies. They are essentially the same for different f_2 frequencies and the amplitude maxima appear at the same frequencies in higher order emissions, although this means that they appear at very different primary ratios f_2/f_1.

It is unlikely that the rippling pattern is generated by the primary mechanisms responsible for the DPOAE generation at the place of primary overlap near the f_2 CF place (Brown and Kemp, 1984). Increase in the overlap of the primaries and shift of their excitation envelopes to the base of the cochlea with increasing the level of stimulation causes a frequency shift, for example, the DPOAE filter functions (Lukashkin and Russell, 2001; Lukashkin *et al.*, 2007) and the DPOAE fine structure (He and Schmiedt, 1993). The local amplitude maxima do not, however, exhibit a level dependent frequency shift. The absence of this frequency shift, along with the frequency invariance of the maxima relative to the f_2, implies that the maxima relate to an amplitude modulation of DPOAE by phenomena related to cochlear structure. This is because any characteristics of the DPOAE governed by mechanisms associated with distortion generation should be strongly influenced by changes in the primary frequency or by changing primary level.

On the other hand, phase of the high-frequency DPOAEs shows oscillations which occur with the same periodicity as the amplitude maxima. Similar phase pattern is usually observed during wave interaction and may indicate generation of the amplitude maxima due to summation of waves at the DPOAE frequencies. In that case, what is the possible origin of these waves? The independence of the local maxima on the frequency of the primary tones makes it unlikely that these maxima are generated by multiple wave interference between distortion-source and reflection-source emissions, which has been used to explain the frequency periodicity of the evoked emissions recorded from the same species in other experiments (Goodman *et al*., 2003; Withnell *et al*., 2003). An additional argument against the local maxima being due to phase interference of emissions from different sources comes from our suppression experiments. DPOAE fine structure has been shown to exist in rodents (Withnell *et al*., 2003), although it presents a cyclic periodicity that is slower than in humans (Talmadge *et al*., 1999, Kalluri and Shera, 2001). If the local maxima and minima were due to a kind of fine structure specific to this species, then placement of the suppressor tone adjacent to the $2f_1$-f_2 would abolish the peak and trough pattern seen in the DPOAE ratio functions presented here. Such observations have been made in humans, where the mechanism responsible for the generation of DPOAE fine structure is widely agreed upon (Heitmann *et al*., 1998; Dhar and Shaffer, 2004). However, the $2f_1$-f_2 signals as a function of the primary ratio described here still show the same peak and trough distribution, in the presence of a suppressor. It therefore follows that the reflection source emissions from the $2f_1$-f_2 CF place are not responsible for the observed local maxima.

Half an octave separation between the local maxima indicate that they may originate from periodic interaction between the basilar membrane and tectorial membrane travelling waves. It is thought that the tectorial membrane is tuned to a frequency about half an octave below the frequency of its cochlea location (Allen, 1980; Gummer *et al*., 1996; Lukashkin *et al*.,

2010) and is capable of maintaining a local travelling wave (Ghaffari *et al*., 2007; Jones *et al*., 2013). Evidence for the half-octave shift in the tectorial membrane tuning comes from mechanical (Gummer *et al*., 1996; Legan *et al*., 2000; Lukashkin *et al*., 2012), acoustic (Allen and Fahey, 1993; Lukashkin and Russell, 2003; Lukashkin *et al*., 2004, 2007) and neural (Liberman, 1978; Allen and Fahey, 1993; Taberner and Liberman, 2005; Russell *et al*., 2007) cochlear responses. The local DPOAE amplitude maxima observed here may relate to this difference in tuning of the basilar and tectorial membranes. Interactions between travelling waves on the tectorial and basilar membranes is, however, a local phenomenon and, hence, should be affected by changes in the f_2 frequency. The local amplitude maxima described here are independent of the primary frequencies and are a global phenomenon associated with propagation rather than generation of energy at the DPOAE frequencies. Therefore, it is unlikely that the tectorial membrane – basilar membrane wave interaction contributes to the generation of the rippling pattern.

Instead, the DPOAE amplitude ripples described here may reflect the formation of standing waves in the cochlea due to multiple internal reflections due to the impedance mismatch at the middle ear boundary (Shera and Zweig, 1991; Russell and Kössl, 1999; Shera, 2003). This multiple wave reflection and interference have been suggested to contribute to generation of DPOAEs (Stover *et al*., 1996; Withnell *et al*., 2003; Dhar and Shaffer, 2004), transient evoked otoacoustic emissions (e.g. Kemp, 1978), stimulus frequency otoacoustic emission (Goodman *et al*., 2003; Berezina-Greene and Guinan, 2015), spontaneous otoacoustic emissions (SOAE) (Kemp, 1979; Russell and Kössl, 1999; Shera, 2003), rippling pattern in basilar membrane responses (Shera and Cooper, 2013) and microstructure in hearing threshold measurements (Shera, 2015). A recent study exploring the suppression pattern of SOAEs in humans (Manley and van Dijk, 2016) found a secondary lobe of suppression located half an octave above the SOAE CF in addition to a V-shaped suppression

region around the CF. It was suggested that the changes in suppression efficacy seen at these points could be due to the suppressor tone nearing nodes and anti-nodes of the SOAE standing wave. The finding reported here that the distance between maxima X, Y and Z is close to half an octave would appear to support the hypothesis that the ripple in the $2f_1$-f_2 amplitude is due to modulation by the SOAE standing wave. The formation of the rippling pattern reported here is due to multiple internal reflections with two provisos. The first is that reflected waves propagate in a linear passive regime. The second is that the boundary conditions, which enable these reflections, do not depend on the non-linear active process. The rippling pattern should then, as we have observed, be independent of stimulus parameters. Within this framework, the rippling is present only in the amplitude and phase of high-frequency DPOAEs because this is favourable for the formation of standing waves. Net energy losses during the round-trip for reflected travelling waves produced by low-frequency primaries, which peak at the cochlear apex, may be too high to support the formation of the standing waves.

SOAEs, which are thought to be produced due to the formation of the standing waves (Kemp, 1979; Russell and Kössl, 1999; Shera, 2003), are far more prominent in humans than in guinea pigs due to the less regular geometry of the primate cochlea (Kemp, 1986; Lonsbury-Martin *et al*., 1988; Shera and Guinan, 1999). Very few examples of independently measured SOAEs in anaesthetised guinea pig exist (Brown *et al*., 1990; Ohyama *et al*., 1991; Nuttall *et al*., 2004). The observation that the frequencies of the local amplitude maxima of DPOAEs are conserved across animals in our experiments may also be due to high levels of anatomical consistency between experimental subjects. The boundary conditions governing formation of the standing waves in guinea pig cochleae could be far less variable, as rodent cochleae are structurally more ordered.

That the presence of standing waves in the rodent cochlea is only suggested by their modulation of the small DPOAE signal is unsurprising. Morphologically regular rodent cochleae do not normally allow generation and emission of high-frequency SOAEs. As a result, these standing waves remain visible only by their interaction with, and influence on DPOAE amplitudes at specific frequencies.

It is worth noting that the DPOAE generation sites are discussed as point sources here and actual generation of the distortion products may occur over an extended region along the cochlea. Hence, it is possible that this extended region can somehow contribute to formation of the rippling pattern of the DPOAE amplitude observed for the high frequency primaries. Regions of interaction between extended source areas should not, however, confound our conclusions.

CONCLUSION

The rippling pattern of high-frequency DPOAE amplitude and corresponding phase oscillations is of cochlear origin and is a global phenomenon associated with propagation rather than generation of energy at the DPOAE frequencies. Frequencies of the local amplitude maxima of the rippling pattern do not depend on parameters of stimulation (i.e. frequency and level of the primaries). The rippling pattern is not suppressed by a third, high-level tone and is likely to originate from multiple internal reflections and formation of standing waves at the DPOAE frequencies within the cochlea.

ACKNOWLEDGMENTS

We thank James Hartley for designing and constructing electronic equipment and Patrício Simões for helpful discussion. The research was funded by a grant from the Medical Research Council [MR/N004299/1].

REFERENCES

Abdala, C., Sininger, Y. S., Ekelid, M., and Zeng, F-G. (**1996**). ‘‘Distortion product otoacoustic emission suppression tuning curves in human adults and neonates,’’ Hear. Res. **98**, 38–53. (DOI:10.1016/0378-5955(96)00056-1)

Allen, J.B. (**1980**). “Cochlear micromechanics – A physical model of transduction,” J. Acoust. Soc. Am. **68**, 1660–1670. (DOI:10.1121/1.385198)

Allen, J. B., and Fahey, P. F. (**1993**). “A second cochlear-frequency map that correlates distortion product and neural tuning measurements,” J. Acoust. Soc. Am. **94**, 809–816. (DOI:10.1121/1.408182)

Avan, P., Büki, B., and Petit, C. (**2013**). “Auditory distortions: origins and functions,” Physiol. Rev. **93**, 1563-1619. (DOI:10.1152/physrev.00029.2012)

Békésy, G. von (**1960**). *Experiments in Hearing* (McGraw-Hill, New York).

Berezina-Greene, M. A., and Guinan, J. J. (**2015**). “Stimulus frequency otoacoustic emission delays and generating mechanisms in guinea pigs, chinchillas, and simulations,” J. Assoc. Res. Otolaryngol. **16**, 679-694. (DOI:10.1007/s10162-015-0543-7)

de Boer, E., Nuttall, A. L., and Shera, C. A. (**2007**). “Wave propagation patterns in a “classical” three-dimensional model of the cochlea,” J. Acoust. Soc. Am. **121**, 352-362. (DOI:10.1121/1.2385068)

Brown, A. M., Gaskill, S. A., and Williams, D. M. (**1992**). “Mechanical filtering of sound in the inner ear,” Proc. R. Soc. B. **250**, 29-34. (DOI:10.1098/rspb.1992.0126)

Brown, A. M., Harris, F. P., and Beveridge, H. A. (**1996**). “Two sources of acoustic distortion products from the human cochlea,” J. Acoust. Soc. Am. **100**, 3260-3267. (DOI:10.1121/1.417209)

Brown, A. M., and Kemp, D. T. (**1984**). "Suppressibility of the $2f_1$-f_2 stimulated acoustic emissions in gerbil and man," Hear. Res. **13**, 29-37. (DOI:10.1016/0378-5955(84)90092-3)

Brown, A. M., Woodward, S., and Gaskill, S. A. (**1990**). "Frequency variation in spontaneous sound emissions from guinea pig and human ears," Eur. Arch. Otorhinolaryngol. **247**, 24-28. (DOI:10.1007/BF00240944)

Dhar, S., and Shaffer, L. A. (**2004**). "Effects of a suppressor tone on distortion product otoacoustic emissions fine structure: Why a universal suppressor level is not a practical solution to obtaining single-generator DP-grams," Ear Hear. **25**, 573-585.

Dieler, R., Shehata-Dieler, W. E., and Brownell, W. E. (**1991**). "Concomitant salicylate-induced alterations of outer hair cell subsurface cisternae and electromotility," J. Neurocytol. **20**, 637– 653. (DOI:10.1007/BF01187066)

Eiber, A., Huber, A. M., Lauxmann, M., Chatzimichalis, M., Sequeira, D., and Sim, J. H. (**2012**). "Contribution of complex stapes motion to cochlea activation," Hear. Res. **284**, 82-92. (DOI:10.1016/j.heares.2011.11.008)

Ghaffari, R., Aranyosi, A. J., and Freeman, D. M. (**2007**). "Longitudinally propagating traveling waves of the mammalian tectorial membrane," Proc. Natl. Acad. Sci. USA **104**, 16510-16515. (DOI:10.1073/pnas.0703665104)

Goodman, S. S., Withnell, R. H., and Shera, C. A. (**2003**). "The origin of SFOAE microstructure in the guinea pig," Hear. Res. **183**, 7-17. (DOI: 10.1016/S0378-5955(03)00193-X)

Greenwood, D. D. (**1990**). "A cochlear frequency-position function for several species—29 years later," J. Acoust. Soc. Am. **87**, 2592-2605. (DOI:10.1121/1.399052)

400 Gummer, A. W., Hemmert, W., and Zenner, H. P. (**1996**). "Resonant tectorial membrane
401 motion in the inner ear: its crucial role in frequency tuning," Proc. Natl. Acad. Sci. USA **93**,
402 8727–8732.

403 Harris, F. P., Probst, R., and Xu, L. (**1992**). ''Suppression of the $2f_1$-f_2 otoacoustic emission in
404 humans,'' Hear. Res. **64**, 133–141. (DOI:10.1016/0378-5955(92)90175-M)

405 He, N. J., and Schmiedt, R. A. (**1993**). "Fine structure of the $2f_1$-f_2 acoustic distortion product:
406 Changes with primary level," J. Acoust. Soc. Am. **94**, 2659-2669. (DOI:10.1121/1.407350)

407 Heitmann, J., Waldmann, B., Schnitzler, H.-U., Plinkert, P. K., and Zenner, H. P. (**1998**).
408 "Suppression of distortion product otoacoustic emissions (DPOAE) near 2f1− f2 removes
409 DP-gram fine structure—Evidence for a secondary generator," J. Acoust. Soc. Am. **103**,
410 1527-1531. (DOI:10.1121/1.421290)

411 Hilger, A. W., Furness, D. N., and Wilson, J. P. (**1995**). "The possible relationship between
412 transient evoked otoacoustic emissions and organ of Corti irregularities in the guinea pig,"
413 Hear. Res. **84**, 1-11. (DOI:10.1016/0378-5955(95)00007-Q)

414 Jones, G. P., Lukashkina, V. A., Russell, I. J., Elliott, S. J., and Lukashkin, A. N. (**2013**).
415 "Frequency-dependent properties of the tectorial membrane facilitate energy transmission
416 and amplification in the cochlea," Biophys. J. **104**, 1357-1366.
417 (DOI:10.1016/j.bpj.2013.02.002)

418 Kalluri, R. and Shera, C. A. (**2001**). "Distortion-product source unmixing: A test of the two-
419 mechanism model for DPOAE generation," J. Acoust. Soc. Am. **109**, 622-637.
420 (DOI:10.1121/1.1334597)

421 Kemp, D. T. (**1978**). "Stimulated acoustic emissions from within the human auditory
422 system," J. Acoust. Soc. Am. **64**, 1386-1391. (DOI:10.1121/1.382104)

Kemp, D. T. (**1979**). "Evidence of mechanical nonlinearity and frequency selective wave amplification in the cochlea," Arch. Otorhinolaryngol. **224**, 37-45. (DOI:10.1007/BF00455222)

Kemp, D. T. (**1986**). "Otoacoustic emissions, travelling waves and cochlear mechanisms," Hear. Res. **22**, 95-104. (DOI:10.1016/0378-5955(86)90087-0)

Kemp, D. T., and Brown, A. M. (**1983**). "An integrated view of cochlear mechanical nonlinearities observable from the ear canal," in *Mechanics of Hearing*, edited by E. de Boer, and M. A. Viergever (Springer, Netherlands), pp. 75-82. (DOI: 10.1007/978-94-009-6911-7_9)

Knight, R. D., and Kemp, D. T. (**2000**). "Indications of different distortion product otoacoustic emission mechanisms from a detailed f_1, f_2 area study," J. Acoust. Soc. Am. **107**, 457-473. (DOI:10.1121/1.428351)

Konrad-Martin, D., Neely, S. T., Keefe, D. H., Dorn, P. A., and Gorga, M. P. (**2001**). "Sources of distortion product otoacoustic emissions revealed by suppression experiments and inverse fast Fourier transforms in normal ears," J. Acoust. Soc. Am. **109**, 2862-2879. (DOI:10.1121/1.1370356)

Kummer, P., Janssen, T., and Arnold, W. (**1995**). ''Suppression tuning characteristics of the $2f_1$-f_2 distortion-product emissions in humans,'' J. Acoust. Soc. Am. **98**, 197–210. (DOI:10.1121/1.413747)

Legan, P. K., Lukashkina, V. A., Goodyear, R. J., Kössl, M., Russell, I. J., and Richardson, G. P. (**2000**). "A targeted deletion in α-tectorin reveals that the tectorial membrane is required for the gain and timing of cochlear feedback," Neuron **28**, 273-285. (DOI:10.1016/S0896-6273(00)00102-1)

Liberman, M. C. (**1978**). "Auditory-nerve response from cats raised in a low-noise chamber," J. Acoust. Soc. Am. **63**, 442–455. (DOI:10.1121/1.381736)

Lonsbury-Martin, B. L., Martin, G. K., Probst, R., and Coats, A. C. (**1988**). "Spontaneous otoacoustic emissions in a nonhuman primate. II. Cochlear anatomy," Hear. Res. **33**, 69-93. (DOI:10.1016/0378-5955(88)90021-4)

Lukashkin, A. N., Legan, P. K., Weddell, T. D., Lukashkina, V. A., Goodyear, R. J., Welstead, L., Petit, C., Russell, I. J., and Richardson, G. P. (**2012**). "A mouse model for human deafness DFNB22 reveals that hearing impairment is due to a loss of inner hair cell stimulation," Proc. Natl. Acad. Sci. USA **109**, 19351–19356. (DOI:10.1073/pnas.1210159109)

Lukashkin, A. N., Lukashkina, V. A., Legan, P. K., Richardson, G. P., and Russell, I. J. (**2004**). "Role of the tectorial membrane revealed by otoacoustic emissions recorded from wild-type and transgenic *Tecta*$^{\Delta ENT/\Delta ENT}$ mice," J. Neurophysiol. **91**, 163-171. (DOI:10.1152/jn.00680.2003)

Lukashkin, A. N., Lukashkina, V. A., and Russell, I. J. (**2002**). "One source for distortion product otoacoustic emissions generated by low-and high-level primaries," J. Acoust. Soc. Am. **111**, 2740-2748. (DOI:10.1121/1.1479151)

Lukashkin, A. N., Richardson, G. P., and Russell, I. J. (**2010**). "Multiple roles for the tectorial membrane in the active cochlea," Hear. Res. **266**, 26-35. (DOI:10.1016/j.heares.2009.10.005)

Lukashkin, A. N., and Russell, I. J. (**1999**). "Analysis of the f2− f1 and 2f1− f2 distortion components generated by the hair cell mechanoelectrical transducer: Dependence on the amplitudes of the primaries and feedback gain," J. Acoust. Soc. Am. **106**, 2661-2668. (DOI:10.1121/1.428096)

Lukashkin, A. N., and Russell, I. J. (**2001**). "Origin of the bell-like dependence of the DPOAE amplitude on primary frequency ratio," J. Acoust. Soc. Am. **110**, 3097-3106. (DOI:10.1121/1.1417525)

Lukashkin, A. N., and Russell, I. J. (**2003**). "A second, low frequency mode of vibration in the intact mammalian cochlea," J. Acoust. Soc. Am. **113**, 1544-1550. (DOI:10.1121/1.1535941)

Lukashkin, A. N., Smith, J. K., and Russell, I. J. (**2007**). "Properties of distortion product otoacoustic emissions and neural suppression tuning curves attributable to the tectorial membrane resonance," J. Acoust. Soc. Am. **121**, 337-343. (DOI:10.1121/1.2390670)

Manley, G. A., and van Dijk, P. (**2016**). "Frequency selectivity of the human cochlea: Suppression tuning of spontaneous otoacoustic emissions," Hear. Res. **336**, 53-62. (DOI:10.1016/j.heares.2016.04.004)

Martin, G. K., Jassir, D., Stagner, B. B., Whitehead, M. L., and Lonsbury-Martin, B. L. (**1998**). "Locus of generation for the 2f1− f2 vs 2f2− f1 distortion-product otoacoustic emissions in normal-hearing humans revealed by suppression tuning, onset latencies, and amplitude correlations," J. Acoust. Soc. Am. **103**, 1957-1971. (DOI:10.1121/1.421347)

Nuttall, A. L., Grosh, K., Zheng, J., De Boer, E., Zou, Y., and Ren, T. (**2004**). "Spontaneous basilar membrane oscillation and otoacoustic emission at 15 kHz in a guinea pig," J. Assoc. Res. Otolaryngol. **5**, 337-348. (DOI:10.1007/s10162-004-4045-2)

Ohyama, K., Wada, H., Kobayashi, T., and Takasaka, T. (**1991**). "Spontaneous otoacoustic emissions in the guinea pig," Hear. Res. **56**, 111-121. (DOI:10.1016/0378-5955(91)90160-B)

Russell, I. J., and Kössl, M. (**1999**). "Micromechanical responses to tones in the auditory fovea of the greater mustached bat's cochlea," J. Neurophysiol. **82**, 676-686.

492 Russell, I. J., Legan, P. K., Lukashkina, V. A., Lukashkin, A. N., Goodyear, R. J., and
493 Richardson, G. P. (**2007**). "Sharpened cochlear tuning in a mouse with a genetically modified
494 tectorial membrane," Nat. Neurosci. **10**, 215-223. (DOI:10.1038/nn1828)

495 Russell, I. J., and Nilsen, K. E. (**1997**). "The location of the cochlear amplifier: Spatial
496 representation of a single tone on the guinea pig basilar membrane," Proc. Natl. Acad. Sci.
497 USA **94**, 2660-2664.

498 Shera, C. A. (**2003**). "Mammalian spontaneous otoacoustic emissions are amplitude-
499 stabilized cochlear standing waves," J. Acoust. Soc. Am. **114**, 244-262.
500 (DOI:10.1121/1.1575750)

501 Shera, C. A. (**2015**). "The spiral staircase: tonotopic microstructure and cochlear tuning," J.
502 Neurosci. **35**, 4683-4690. (DOI:10.1523/JNEUROSCI.4788-14.2015)

503 Shera, C. A., and Cooper, N. P. (**2013**). "Basilar-membrane interference patterns from
504 multiple internal reflection of cochlear traveling waves," J. Acoust. Soc. Am. **133**, 2224-
505 2239. (DOI:10.1121/1.4792129)

506 Shera, C. A., and Guinan, J. J. (**1999**). "Evoked otoacoustic emissions arise by two
507 fundamentally different mechanisms: A taxonomy for mammalian OAEs," J. Acoust. Soc.
508 Am. **105**, 782-798. (DOI:10.1121/1.426948)

509 Shera, C.A., and Zweig, G. (**1991**). "Reflection of retrograde waves within the cochlea and at
510 the stapes," J. Acoust. Soc. Am. **89**, 1290-1305. (DOI:10.1121/1.400654)

511 Stover, L. J., Neely, S. T., and Gorga, M. P. (**1996**). "Latency and multiple sources of
512 distortion product otoacoustic emissions," J. Acoust. Soc. Am. **99**, 1016-1024.
513 (DOI:10.1121/1.414630)

514 Taberner, A. M., and Liberman, M. C. (**2005**). "Response properties of single auditory nerve
515 fibers in the mouse," J. Neurophysiol. **93**, 557–569. (DOI:10.1152/jn.00574.2004)

516 Talmadge, C. L., Long, G. R., Tubis, A., and Dhar, S. (**1999**). "Experimental confirmation of
517 the two-source interference model for the fine structure of distortion product otoacoustic
518 emissions," J. Acoust. Soc. Am. **105**, 275-292. (DOI:10.1121/1.424584)

519 Vetešník, A., and Gummer, A. W. (**2012**). "Transmission of cochlear distortion products as
520 slow waves: A comparison of experimental and model data," J. Acoust. Soc. Am. **131**, 3914-
521 3934. (DOI:10.1121/1.3699207)

522 Withnell, R. H., Shaffer, L. A., and Talmadge, C. L. (**2003**). "Generation of DPOAEs in the
523 guinea pig," Hear. Res. **178**, 106-117. (DOI:10.1016/S0378-5955(03)00064-9)

524 Zweig, G., and Shera, C. A. (**1995**). "The origin of periodicity in the spectrum of evoked
525 otoacoustic emissions," J. Acoust. Soc. Am. **98**, 2018-2047. (DOI:10.1121/1.413320)